BMC Oral Health

RESEARCH

Open Access

Fibrin-konjac glucomannan-black phosphorus hydrogel scaffolds loaded with nasal ectodermal mesenchymal stem cells accelerated alveolar bone regeneration

Yin Zou[1], Xue Mei[2], Xinhe Wang[2], Xuan Zhang[2], Xun Wang[3], Wen Xiang[4] and Naiyan Lu[2*]

Abstract

Background Effective treatments for the alveolar bone defect remain a major concern in dental therapy. The objectives of this study were to develop a fibrin and konjac glucomannan (KGM) composite hydrogel as scaffolds for the osteogenesis of nasal mucosa-derived ectodermal mesenchymal stem cells (EMSCs) for the regeneration of alveolar bone defect, and to investigate the osteogenesis-accelerating effects of black phosphorus nanoparticles (BPNs) embedded in the hydrogels.

Methods Primary EMSCs were isolated from rat nasal mucosa and used for the alveolar bone recovery. Fibrin and KGM were prepared in different ratios for osteomimetic hydrogel scaffolds, and the optimal ratio was determined by mechanical properties and biocompatibility analysis. Then, the optimal hydrogels were integrated with BPNs to obtain BPNs/fibrin-KGM hydrogels, and the effects on osteogenic EMSCs in vitro were evaluated. To explore the osteogenesis-enhancing effects of hydrogels in vivo, the BPNs/fibrin-KGM scaffolds combined with EMSCs were implanted to a rat model of alveolar bone defect. Micro-computed tomography (CT), histological examination, real-time quantitative polymerase chain reaction (RT-qPCR) and western blot were conducted to evaluate the bone morphology and expression of osteogenesis-related genes of the bone regeneration.

Results The addition of KGM improved the mechanical properties and biodegradation characteristics of the fibrin hydrogels. In vitro, the BPNs-containing compound hydrogel was proved to be biocompatible and capable of enhancing the osteogenesis of EMSCs by upregulating the mineralization and the activity of alkaline phosphatase. In vivo, the micro-CT analysis and histological evaluation demonstrated that rats implanted EMSCs-BPNs/fibrin-KGM hydrogels exhibited the best bone reconstruction. And compared to the model group, the expression of osteogenesis genes including osteopontin (*Opn*, $p < 0.0001$), osteocalcin (Ocn, $p < 0.0001$), type collagen (Col , $p < 0.0001$), bone morphogenetic protein-2 (Bmp2, $p < 0.0001$), Smad1 ($p = 0.0006$), and runt-related transcription factor 2 (Runx2, $p < 0.0001$) were all significantly upregulated.

*Correspondence:
Naiyan Lu
lunaiyan@jiangnan.edu.cn

Full list of author information is available at the end of the article

Conclusions EMSCs/BPNs-containing fibrin-KGM hydrogels accelerated the recovery of the alveolar bone defect in rats by effectively up-regulating the expression of osteogenesis-related genes, promoting the formation and mineralisation of bone matrix.

Keywords Fibrin, Konjac glucomannan, Black phosphorus, Ectodermal mesenchymal stem cells, Alveolar bone defect

Background

The alveolar bone, one of the supporting tissue of the tooth root, is essential for the growth and maintenance of teeth [1]. Caused by periodontitis, external-force injuries, and maxillofacial dysplasia [2], the alveolar bone defect has become a major concern in dental therapy. Bone grafting is commonly used during the treatment of alveolar bone defects, and the autologous bone is thought to be the gold standard graft material [3, 4]. However, the harvest of autologous bone may cause additional harm to the patient, with high rates of complications [5]. Allogeneic bone is another source of bone graft, but it comes with a high risk of immunogenicity [6] and inferior healing effects [7]. The other treatment for alveolar bone defect is distraction osteogenesis, which stimulates the growth of bone and the overlaying soft tissues through gradual and incremental traction, but is also accompanied by complications and the risk of reoperation [8–10].

To avoid those limitations, bone tissue engineering has developed gradually over the years. The establishment of a successful bone substitute requires three key components: bioactive scaffolds, cytokines, and seed cells [11, 12]. However, most of the traditional synthetic polymers are hydrophobic and fast-biodegradable, limiting their ability to encapsulate cells and regeneration of bone tissue in a long-term process [13, 14]. Some trace elements or bioactive substances could promote the formation of extracellular matrix and the biomineralization processs [15]. The currently-used bone mineration materials such as calcium carbonate [16] and calcium phosphate [17], show an uncontrollable release of phosphate and possess high hardness which makes it difficult to fit the defect region [18]. In adddition, bone formation mainly depends on the osteogenic potential and proliferative capability of endogenous or exogenous bone marrow mesenchymal stem cells (BMSCs), but the limited proliferative ability and high invasion operation restricted their application in clinical settings [10, 11]. Therefore, there is a need for a right combination of bio-friendly materials and cell source to overcome these limitations in bone tissue engineering.

The ectodermal mesenchymal stem cells (EMSCs) have been considered an ideal seed cell for bone tissue engineering due to easy acquisition, noninvasiveness and high osteogenic potential [19]. EMSCs derived from the neural crest have attracted great interest due to the easy availability from the nasal mucosa [20]. Nasal mucosal ectodermal EMSCs showed multidirectional differentiation potential, such as osteoblasts [21]. In addition, EMSCs can secrete cytokines and growth factors that contributed to bone regeneration [22]. Our previous study showed that bone-like grafts loaded with EMSCs presented good repair effects for cranial defects [23]. However, it remains unknown whether nasal mucosa-derived EMSCs can be used as seed cells to effectively repair alveolar bone damage. Therefore, nasal mucosa-derived EMSCs were applied to alveolar bone defects to verify the repair potential. In addition to seed cells, bone substitutes required bioactive scaffolds to realise their osteogenic potential. Fibrin scaffolds carrying MSCs possessed considerable potential for application in bone repair and regeneration, and the addition of KGM may slow down the degradation of fibrin hydrogels [24, 25] and form an appropriate extracellular environment for the growth and proliferation of stem cells. In this study, we prepared bone biomimetic hydrogel scaffolds of fibrin and konjac glucomannan (KGM) in varying proportions and the optimal ratio was determined through analysis of the mechanical properties and biocompatibility. Based on the good osteogenesis-promoting capacity of black phosphorus nanoparticles (BPNs) in our previous study [26], the optimum hydrogels were then integrated with BPNs to obtain BPNs/fibrin-KGM hydrogels, and their effects on EMSCs of osteogenesis in vitro were evaluated. A rat model of alveolar bone defect was used to assess the effects of the scaffolds placed EMSCs on bone repair. Our study demonstrated the potential usage of BPNs/fibrin-KGM-EMSCs composite hydrogels in the clinical treatment of alveolar bone defects.

Methods

Isolation, culture, and verification of EMSCs

The experimental design of this study is shown in Fig. 1. Firstly, the primary EMSCs were isolated from the nasal mucosa of rats [19]. In short, two four-week-old Sprague Dawley rats provided by Jiangnan University were euthanatized via CO_2 asphyxiation, followed by cervical dislocation for physical confirmation of euthanasia. After adequate disinfection, the middle third of the nasal septum was carefully dissected from the rats, washed with phosphate buffer saline (PBS) twice, and then minced into pieces. The pieces of nasal septum were incubated in a 0.25% trypsin solution (Gibco, Carlsbad, CA, USA) at 37℃ for 30 min. The trypsin-digested pieces were planted into a cell culture flask and cultured with Dulbecco's modified Eagle's medium/nutrient mixture F12

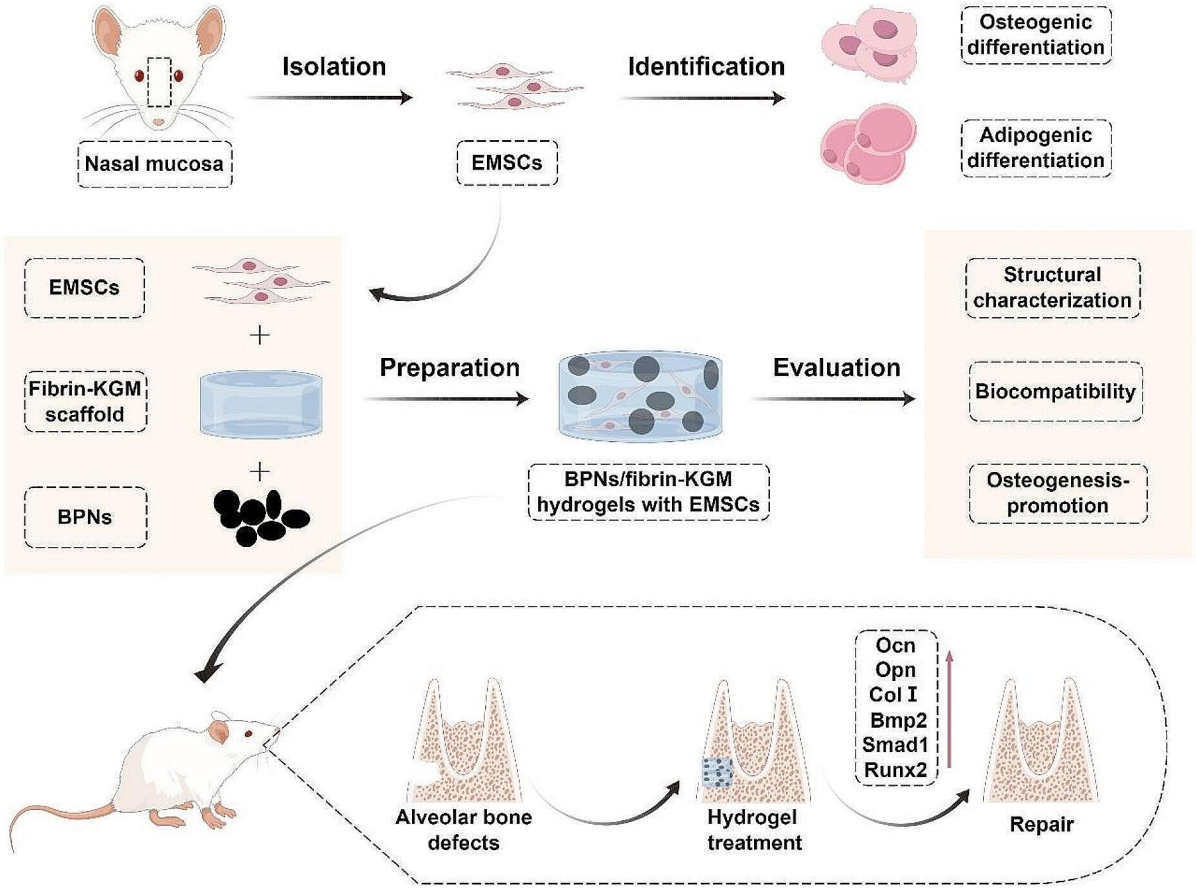

Fig. 1 The experimental design of this study

(DMEM/ F12) medium (Hyclone, UT, USA) containing 10% fetal bovine serum (FBS, Gibco), 100 U/mL penicillin, and 100 μg/mL streptomycin (Biyuntian Biotechnology, Shanghai, China) in an incubator (Thermo Fisher Scientific, CA, USA) at 37℃, 5% CO_2 and 95% air humidity. The medium was replaced every three days, and the cells were passaged until reaching 90% confluence. Cells in the third passage were used for further study.

Immunofluorescence was performed to detect neural crest cell markers and stem cell markers. The third-passage EMSCs inoculated on cell climbing slices were fixed with 4% paraformaldehyde (Biyuntian) for 20 min at room temperature and the cells were incubated with primary antibodies against various cell markers including nestin, vimentin, and snail (Proteintech, Wuhan, China). The slices were then taken out and immunofluorescent stained with fluorescein isothiocyanate (FITC)-conjugated goat anti-rabbit secondary antibody (Proteintech). The slices were examined with an inverted fluorescence microscope (Axio Vert A1, Zeiss, Germany).

Identification of the multi-directional differentiation ability of EMSCs

The EMSCs at passage three were seeded in 6-well plates. When the cells reached 70% confluence (for osteogenic differentiation) or 90% confluence (for adipogenic differentiation), the medium was replaced with osteogenic differentiation medium including 10% FBS, 0.1 mM dexamethasone (Aladdin), 10 mM β-glycerophosphate disodium (Sinopharm, Wuhan, China), and 0.2 mM L-ascorbic acid (Sinopharm) or adipogenic differentiation medium(Gibco) to induce osteogenesis or adipogenesis, respectively. The medium was changed every 3 days and Alizarin red S (ARS) staining (Biyuntian) was performed on day 14 to estimate the deposition of calcium phosphate. Oil Red staining (Biyuntian) was conducted on day 14 according to the manufacturer's recommendations to detect intracellular lipid accumulation.

Synthesis and characterization of BPNs

The BPNs were exfoliated from bulk BP (Nanjing XFNANO Materials, Nanjing, China) through an improved liquid phase stripping method [27]. In brief, 20 mg bulk BP was immersed in 20 mL

N-methyl-2-pyrrolidone (Aladdin, Shanghai, China) and sonicated in the ice bath for 8 h. The obtained dark grey suspension was then centrifuged at 4000 rpm for 15 min to remove the large unexfoliated BP. Then, further centrifugation of the supernatant was performed at 15,000 for 15 min, and the precipitate was collected, washed, re-centrifuged twice with deionized water, and vacuum desiccated to obtain BPNs in powder form.

The morphology and size of BPNs were evaluated by scanning electron microscope (SEM). The BPNs solution at a concentration of 1 mg/mL in deionized water was dropped onto a thin copper sheet and then air dried. Samples were photographed by SEM (H-7500 Hitachi, Tokyo, Japan). The mean size of the BPNs was analyzed by Image Pro Plus software (Media Cybernetics, MD, USA). The size distribution of BPNs was evaluated by the particle sizer Zetasizer nano ZS.

Fabrication and characterization of the fibrin-KGM scaffold

KGM (Hefei Bomei Biotechnology, Hefei, China) was purified according to previous studies [28]. The KGM flour was stirred with 70% ethanol and then centrifuged at 4000 rpm for 20 min, washed with absolute ethanol for three times, and then vacuum dried.

The purified KGM was dissolved in 0.50% (w/v) Na_2CO_3 solution to prepare a KGM solution by stirring at 800 rpm for 4 h to achieve complete deacetylation. Fibrinogen (Shenyang Baiying Biotechnology, Shenyang, China) was dissolved in PBS. The fibrinogen solution was mixed well with an equal amount of thrombin (Shenyang Baiying Biotechnology), and then mixed with the KGM solution to prepare composite hydrogels according to Table 1. The composite hydrogels were incubated at 37 °C for 30 min for the formation and stabilization of the structure of fibrin gels, heated for 30 min, and then refrigerated for 24 h at 4 ℃ in the refrigerator to form gels.

To determine the degradation rate of the composite gel in vitro, the hydrogel samples were immersed in PBS and cultured in an incubator at 37℃. The solution was refreshed every 24 h. The surface water of the hydrogels was dried by the filters at each measurement time point. The gel characteristic was evaluated according to Fan Rui's method [29]. The texture characteristics of the hydrogels were determined by a texture analyzer (TA.XT Plus, SMS, Britain). The texture profile analysis mode and probe P 0.5 were selected for testing. The parameters of the test were: pre-test speed 2 mm/s, test speed 1 mm/s, compression distance 10 mm, and trigger force 5 g.

Cytocompatibility of BPNs/fibrin-KGM hydrogels with EMSCs

The proliferation of EMSCs on fibrin-KGM scaffolds was evaluated with the cell counting kit-8 (CCK-8, Biyuntian). EMSCs were plated in the hydrogel-coated 96-well plates (3000 cells per well) and cultured in DMEM/F12 medium for 48 h in an incubator, while EMSCs planted in the 96-well plates were set as the control group. According to the manufacturer's instructions, 20 μL CCK-8 reagent was added to the medium and incubated at 37℃ for 1 h. Optical density (OD) at 450 nm was measured with the microplate reader.

To access the growth of EMSCs o-n the surface of the composite hydrogels, EMSCs were inoculated in the 12-well plates coated with the fibrin-KGM hydrogels and cultured in a complete culture medium for 48 h. The cells were stained with calcein acetoxymethyl ester and propidium iodide (Calcein-AM and PI, Biyuntian) to discriminate between viable cells and dead ones. Calcein-AM is capable of staining viable cells green, while PI stains dead cells red owing to its inability to penetrate the cell membrane. Fluorescent images were captured by the fluorescence microscope.

Characterization of the BPNs/fibrin-KGM hydrogels

According to our previous study, BPNs were mixed with the optimal proportion of hydrogels at a concentration of 4 μg/mL [26]. To determine the effects of the addition of BPNs on the properties of the composite hydrogels, the water-holding capacity (WHC), texture characteristics, and cytocompatibility of the BPNs/fibrin-KGM hydrogels were accessed.

Osteogenic differentiation of EMSCs on the BPNs/fibrin-KGM hydrogels

The BPNs/fibrin-KGM hydrogels were prepared in 6-well plates as described previously, with EMSCs seeded and cultured in a complete medium till 70% confluence. The medium was then changed to an osteogenic differentiation medium without β-glycerophosphate disodium to avoid the disturbance of exogenous phosphorus sources. Alkaline phosphatase (ALP) staining (Biyuntian) was conducted on day 7 according to the manufacturers' instructions. On day 14, ARS was employed to determine the presence of calcium deposits. Briefly, after being fixed with fixation solution for 30 min, the cells on hydrogels were stained with Alizarin red S solution for 1 h. Then, the cells were washed three times with deionized water

Table 1 Concentrations of fibrin and KGM in the composite gel

	NF	FK_1	FK_2	FK_3	FK_4	NK
Fibrin% (w/v)	2.0	1.6	1.2	0.8	0.4	0.0
KGM% (w/v)	0.0	0.4	0.8	1.2	1.6	2.0

and observed under the microscope. Image analysis was conducted with Image Pro Plus.

Establishment of alveolar bone defect models in rats

The protocol of the animal study was in accordance with the National Institutes of Health guidelines and approved by Jiangnan University Animal Care and Ethics Committee. Six-week-old male Sprague Dawley rats (200 g) were anesthetized with 1% pentobarbital sodium (40 mg/kg) and 1% lidocaine was injected near the surgery site to minimize incision pain. Under sterile conditions, the gingiva close to the first upper molar was cut open to expose the operation area [30]. An alveolar bone defect of 2 mm in diameter was prepared with a high-speed dental drill with saline flushing to keep the low temperature of surgical areas. The EMSCs (5×10^5 cells per well) were seeded on the hydrogels in the 6-well plates three days before the surgery. Fibrin-KGM hydrogels/ EMSCs-fibrin-KGM hydrogels/ BPNs-EMSCs-fibrin-KGM hydrogels were implanted in the defect region of three groups of experimental rats ($n=6$ for each group). A model group sutured directly with nothing implanted was also set. The incision was then carefully closed with a 7−0 silk suture. A standard diet was provided for the rats and local swelling or redness or any negative effects on eating were observed every day after the surgery.

Micro-CT analysis

Animals from three experimental groups and one model group were sacrificed 4 weeks after the surgery. The whole maxillae were isolated with soft tissues removed and washed twice with PBS. Immersed in 75% ethanol, the samples were scanned with the IVIS SPECTRUM micro-computed tomography (micro-CT) system (Perkin Elmer, USA). A three-dimensional reconstruction of the maxillae was generated. The defect areas were selected as the region of interest (ROI), with bone mineral density (BMD) and trabecular parameters of the ROI analyzed.

Histological evaluation

After euthanasia, the target region of maxillae was isolated from the mandible, immersed in 4% paraformaldehyde for 24 h, and then incubated in 10% ethylenediaminetetraacetic acid (Sinopharm) decalcified solution at 4℃ for four weeks, with the supernatant changed every three days. Once the decalcification was complete, the samples were washed in flowing water for 12 h, dehydrated with gradient ethanol, and embedded into the paraffin. The wax blocks were sectioned at a thickness of 6 μm in the sagittal direction along the bone defect. After the sections were deparaffinized and hydrated, hematoxylin-eosin staining (H&E staining, Biyuntian) was conducted according to the manufacturer's protocols.

Table 2 Gene primers

Gene	Forward primers (5′-3′)	Reverse primers (5′-3′)
Ocn	TCCAATGAAAGCCATGACCAC	ATTCGTCAGATTCATCCGAGT
Opn	GCAAAGCCCAGCGACTCTGA	TAGCGCCGGAGTCTATTCACC
Col	ACTGGTACATCAGCCCAAACCC	ACTCGAACTGGAATCCAT CGGT
Bmp2	CATCACGAAGAAGCCATCGAG	TTCCTGCATTTGTTCCCGAA
Smad1	TTTCATCCCACCACGGTCTGC	CCCAGCCCTTCACGAAGCTC
Runx2	GCACGACCACCTCGAATGGC	GGCTTCCATCAGCGTCAA CACC
Gapdh	TATGACTCTACCCACGGCAAG	ATACTCAGCACCAGCATCACC

RT-qPCR and Western blot analysis

The real-time quantitative polymerase chain reaction (RT-qPCR) was carried out to evaluate the gene expression of osteogenesis-related genes. A rapid RNA extraction kit for bone tissue (Aidlab Biotechnologies, Beijing, China) was used to extract the total RNA of bone tissue. The Reverse-Transcriptase Kits (Vazyme Biotech, Nanjing, China) were utilized for the synthesis of cDNA and SYBR Green Kits (Vazyme) were used to quantify gene expression levels. Primers used for RT-qPCR were synthesized by Genewiz Biotechnology Co., Ltd (Suzhou, China). The primer sequences are listed in Table 2. The expression levels of mRNA were normalized to the expression level of glyceraldehyde-3-phosphate dehydrogenase (*Gapdh*), and the mean values were calculated based on the formula $2^{-\Delta\Delta Ct}$.

Western blot was conducted to determine the differences in the expression of osteogenesis-related proteins between different experimental groups. The maxilla tissues were kept in ice-cold PBS, and the total protein of the maxillae was extracted with a bone tissue protein extraction kit (Beijing Baiaolaibo, Beijing, China). The lysates were harvested by centrifugation at 13,000 g for 10 min at 4℃ and diluted with the loading buffer (Biyuntian). Protein content was determined with a protein quantitative kit (Biyuntian). After volume normalization, the extracted proteins were separated by 10% sodium dodecyl sulfate-polyacrylamide gel electrophoresis (SDS-PAGE, Invitrogen, NY, USA) and transferred onto polyvinylidene fluoride (PVDF) membranes (Invitrogen). The membranes were blocked by 5% bovine serum albumin in 0.01 M Tris-buffered saline with 0.2% Tween (TBS-T, Solarbio) at room temperature for 1.5 h. The primary antibodies (Proteintech) against type collagen (COL, 1:1000), runt-related transcription factor 2 (RUNX2, 1:1000), and BMP2 (1:1000), with GAPDH used as the internal reference protein, were incubated with the membranes at 4℃ overnight. Then the membranes were incubated with peroxidase-conjected secondary antibodies (goat anti-rabbit-IgG, 1:10000) on a shaker at room temperature for 1 h. The results were detected using the

enhanced electrochemiluminescence (ECL) kit (Biyuntian) on the Tanon-5200 Chemiluminescent Imaging System (Tanon Science and Technology, Shanghai, China).

Statistical analysis

The statistical analysis was performed with Origin pro software (2018, OriginLab). All the data were expressed as mean ± standard deviation (SD) and multiple groups statistical analyses were performed by one-factor analysis of variance (ANOVA) tests. The data with p-value < 0.05 were considered statistically significant.

Results

Isolation and characterization of EMSCs

The cultured EMSCs at the third passage were relatively homogenous with flattened morphology similar to fibroblastic cells and proliferated well on plastic plates (Fig. 2A). The EMSCs were differentiated into osteogenic cells in an osteogenic medium and stained by Alizarin red S staining. The adipogenic differentiation of EMSCs in an adipogenic-induction medium was assessed by Oil red-O staining. High rates of the positive area were observed in both Alizarin red S (Fig. 2B) and Oil red-O staining (Fig. 2C). The cultured cells expressed neural crest cell and stem cell markers including nestin (Fig. 2D), vimentin (Fig. 2E), and snail (Fig. 2F) strongly.

Preparation and characterization of BPNs and fibrin-KGM hydrogels

BPNs were exfoliated from bulk black phosphorus by the liquid exfoliation method. SEM was carried out to characterize the morphology and measure the particle size of BPNs (Fig. 3A, B). The size distribution of BPNs evaluated by the particle sizer (Fig. 3C) illustrated that the BPNs were exfoliated from bulk BP successfully, with the particle size ranging from 60 to 120 nm.

The fibrin-KGM hydrogels were prepared and characterized. The biodegradation of fibrin-KGM hydrogels in vitro was investigated (Fig. 3D). The retention rate of hydrogels with high content of KGM was higher than 60% after 21 days of immersing in PBS at 37℃, while the fibrin hydrogel degraded completely before day 7.

For bone-tissue engineering and cell culture, the scaffolds should possess adequate mechanical properties and good water-holding capacity. A TAPlus texture analyzer was used to detect the gel strength of the hydrogels.

With the increase of the proportion of KGM, the gel strength and the WHC of the composite gel increased first and then decreased, and reached the maximum when the concentration of KGM was 1.6% (w/v) and the concentration of fibrin was 0.4% (w/v). Compared with fibrin gel, the fibrin-KGM composite gel showed better gel strength and ability of water retention (p < 0.0001, group NF vs. group FK_4, Fig. 3E).

Biocompatibility evaluation between fibrin-KGM hydrogels and EMSCs

To determine the biocompatibility of fibrin-KGM hydrogels, EMSCs were planted to the hydrogels and cultured in DMEM/F12 medium for 3 days. The relative viability rates of the EMSCs were assessed by a CCK-8 kit. The results (Fig. 4A) indicated that the OD values firstly

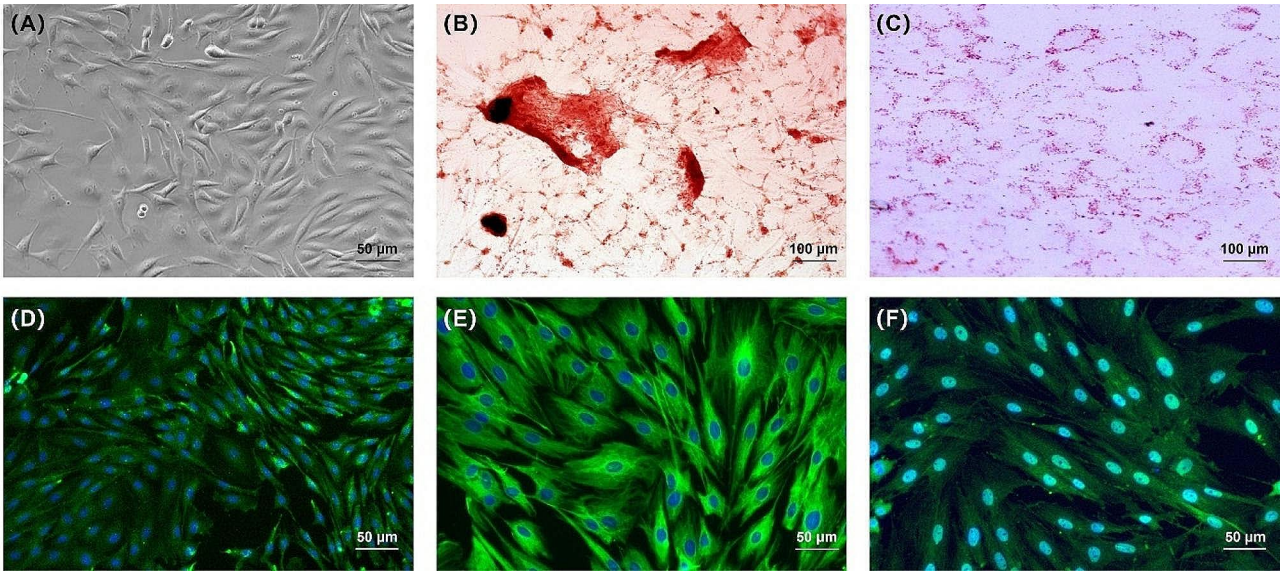

Fig. 2 Culture and identification of EMSCs. (**A**) EMSCs at the third passage were relatively homogenous with flattened morphology similar to fibroblastic cells. (**B**, **C**) Cultured in the corresponding medium for 21 days, EMSCs were differentiated into osteocytes (**B**) and adipocytes (**C**) cells. (**D**) Expression of neural crest cell markers, including nestin, vimentin, and snail, was assessed by immunofluorescence staining. The IgG-FITC (green) was used as the secondary antibody for the immunofluorescence staining and the nuclei were stained with 4′,6-diamidino-2-phenylindole (DAPI, blue)

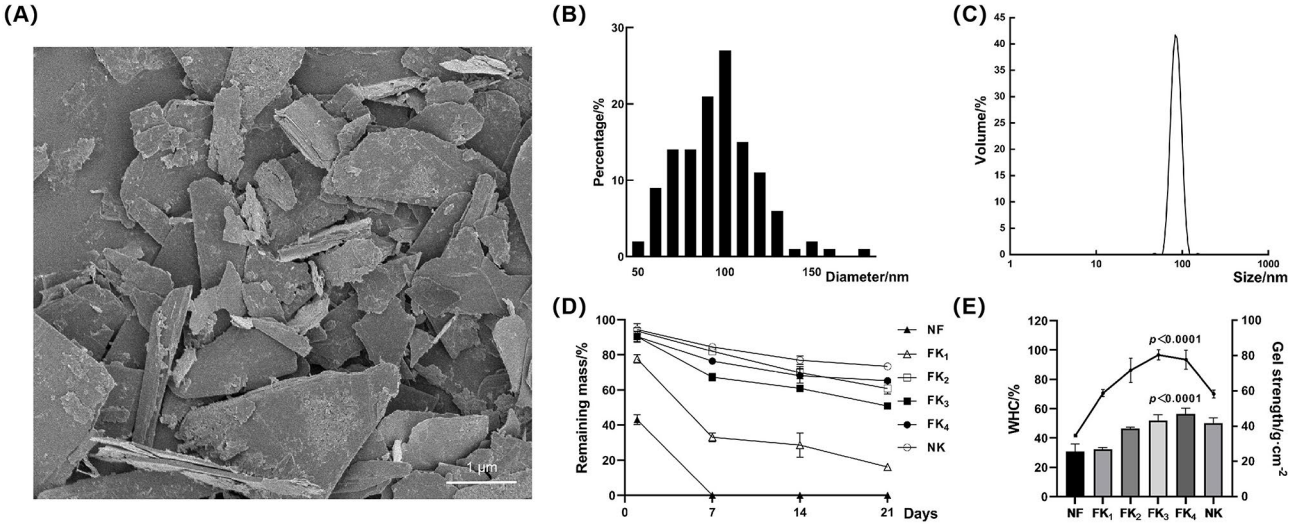

Fig. 3 Characterization of BPNs and fibrin-KGM hydrogels. **(A)** SEM image of BPNs. (**B**, **C**) Measurement of the particle size of BPNs. **(D)** Degradation rate in vitro of fibrin-KGM hydrogels. **(E)** Water-holding capacity (WHC, the line graph) and gel strength(the column graph) of fibrin-KGM hydrogels. Data were presented as mean ± standard deviation (SD), $n=3$. (group NF vs. group FK_4)

increased and then decreased with the increase in the proportion of KGM ($p=0.0038$, group Con vs. group FK_4). The OD values of the NK group decreased compared with the control group, though it was not statistically significant. To further confirm the effects of the fibrin-KGM hydrogels on the cell viability of EMSCs, Calcein-AM, and PI staining assays were used to characterize live cells and dead cells in green and red fluorescence, respectively (Fig. 4B). Similar to the results of CCK-8, there was a trend to increase of the amounts of viable cells with increases in the proportion of KGM in the NF, FK_1, FK_2, and FK_3 groups. The majority of cells for all groups were alive except the NK group. In general, pure NK has some cytotoxicity, which could be reduced by the blending of KGM and fibrin. FK_3 showed the best effects in reducing cytotoxicity and promoting proliferation. Therefore, the FK_3 hydrogel was used for further study, because of its excellent biocompatibility, moderate degradation rate, and fine gel properties.

Evaluation of the effects of BPNs on the gel properties and bicompaitbility of fibrin-KGM hydrogels

The WHC, gel strength, and biocompatibility of the BPNs/fibrin-KGM hydrogels were determined to evaluate the effects of the addition of BPNs. The results indicated that compared with the fibrin-KGM hydrogels, the addition of BPNs had no significant effects on the gel properties and cytocompatibility of the composite hydrogels (Fig. 5A-C).

Osteogenesis of EMSCs on BPNs/fibrin-KGM hydrogels

To confirm the effects of compound hydrogels on the osteogenesis of EMSCs, ALP (Fig. 6A) and ARS (Fig. 6B) staining were conducted to identify the expression of ALP and calcium nodules. After 7 days, the EMSCs co-cultured with BPNs and BPNs/fibrin-KGM hydrogels showed a significant increase ($p=0.0022$, group Con vs. group BPNs; $p=0.0003$, group Gel vs. group BPNs/Gel) in the expression of ALP, with no obvious difference observed between those two groups (Fig. 6C). The ARS staining was conducted after 14 days of induction. The EMSCs cultured on the fibrin-KGM hydrogel formed unshaped calcium nodules, while the mineralized nodules of the BPNs-treated EMSCs were much larger ($p=0.0011$, group Con vs. group BPNs; $p=0.0014$, group Gel vs. group BPNs/Gel) compared with the control group (Fig. 6D). These results tentatively indicated that the BPNs/fibrin-KGM hydrogels had a positive effect on the osteogenesis of EMSCs.

The effects of BPNs/fibrin-KGM hydrogels on bone regeneration in vivo

The BPNs/fibrin-KGM hydrogels were implanted in the alveolar bone defect rats, and the rats were sacrificed after 4 weeks. The maxillary bone tissues were collected for micro-CT. The micro-CT analysis indicated that the area of bone defect in the EMSCs/gel and BPNs-EMSCs/gel groups was smaller than that in the model group and hydrogel group (Fig. 7A). In addition, the bone histomorphometric analysis revealed that the BMD, bone volume (BV), bone volume fraction (BV/TV), and trabecular thickness (Tb. Th) of the BPNs-EMSCs/gel group were significantly higher than that of the model group (Fig. 7B-E). H&E staining was also conducted to determine the bone regeneration of the experimental and model groups (Fig. 8). Histological analysis indicated that the rats treated with EMSCs-containing hydrogels produced relatively mature bone with consecutive bone structure and

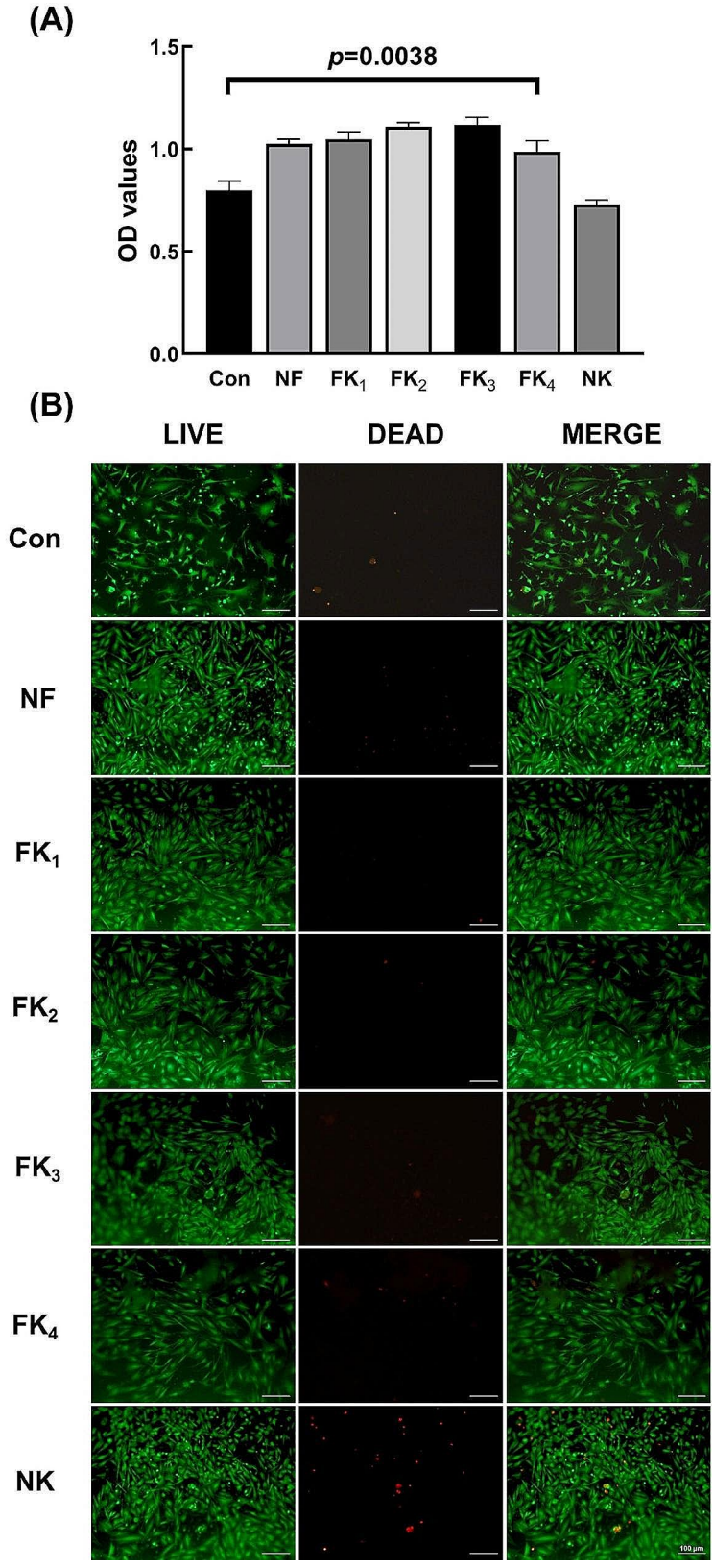

Fig. 4 The cytocompatibility of the fibrin-KGM hydrogels. **(A)** The cytotoxicity of fibrin-KGM hydrogels was determined by the CCK-8 kit. Data were presented as mean ± standard deviation (SD), $n = 6$. **(B)** Live/dead staining assay was conducted to evaluate the cytocompatibility of the hydrogels. The live cells were stained green while the dead cells were stained red

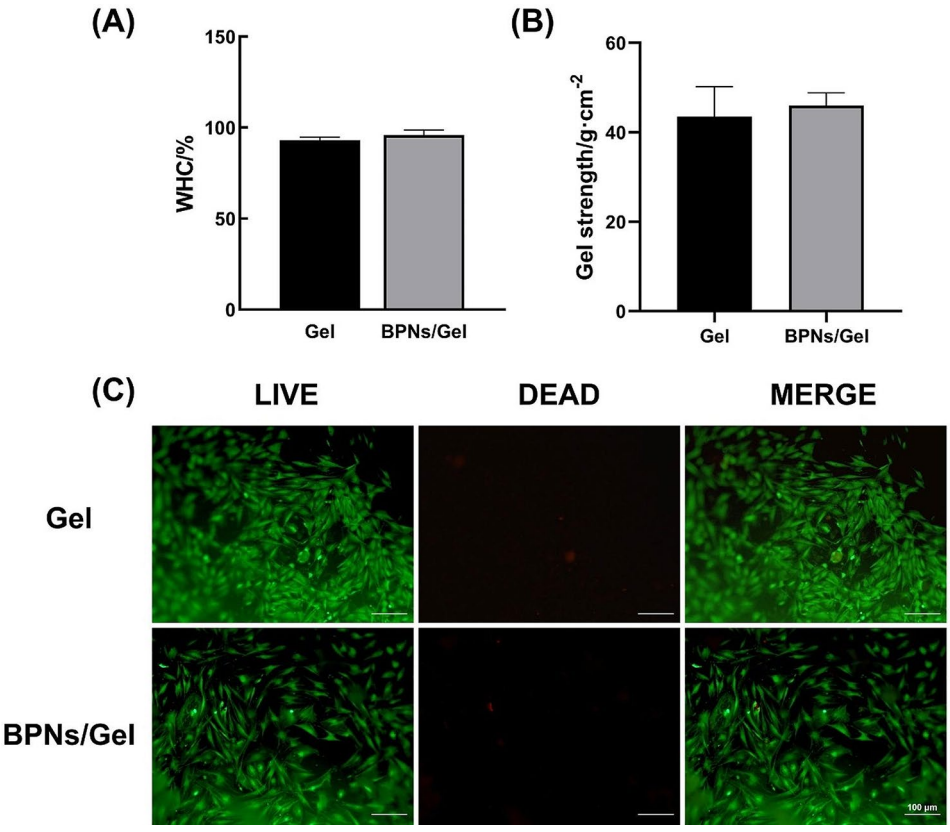

Fig. 5 The gel properties and biocompatibility of the BPNs/fibrin-KGM hydrogels. (**A**, **B**) The WHC and gel strength of the fibrin-KGM hydrogels and the BPNs/fibrin-KGM hydrogels. Data were presented as mean ± standard deviation (SD), $n = 3$. **(C)** A live/dead staining assay was used to evaluate the biocompatibility of the hydrogels and the BPNs-containing hydrogels

orderly bone trabeculae, while few mature bones were observed in the model group and hydrogel-treated.

group. Moreover, the construction of vascular structures was more active in the BPNs-EMSCs/gel group, with more new vessels observed.

Osteogenesis-related mRNA and protein expression

Compared with the model group, the mRNA expression levels of osteopontin (*Opn*), osteocalcin (*Ocn*), *Col*, *Bmp2*, *Smad1*, and *Runx2* were all significantly upregulated in the BPNs/EMSCs-gel group (Fig. 9A). Consistently, western blot analysis demonstrated upregulated protein expression of COL, BMP2 and RUNX2 the EMSCs-gel group and BPNs/EMSCs-gel sheets group (Fig. 9B). These results indicated that the BPNs/EMSCs-containing hydrogels could promote the alveolar bone regeneration.

Discussion

Despite the rapid development of bone tissue engineering, the effective regeneration of bone tissue remains a huge challenge due to the complexity of the microenvironment of the defect area [31]. An ideal scaffold with proper mechanical properties and biocompatibility is a significant part of bone tissue engineering [32, 33]. Hard materials such as polymers, metals, and carbon-based ceramics [34] have been widely utilized as bioactive scaffolds, though come with the disadvantages of poor mechanical properties and slow resorption rates [35]. Hydrogels have received extensive attention in these years since the network structures of hydrogels are remarkably similar to the protein-polysaccharide-based networks of ECM.

In this study, a bone tissue engineering scaffold was prepared by polysaccharides and proteins of food origin, incorporated with BPNs. The fibrin-KGM composite hydrogels were proven to support the proliferation and osteogenesis of EMSCs in vitro. The alveolar bone defect model of rats was constructed, and the results of Micro-CT, histological analysis, RT-qPCR, and Western blot demonstrated the great potential of EMSCs-loaded BPNs/fibrin-KGM hydrogels in bone regeneration.

Fibrin offers unique advantages for its multiple interaction sites for cells [36], and has been widely used in bone tissue engineering [19, 37]. Researchers have investigated the effects of fibrin hydrogels in the regeneration of cranial defects [38], femur defects [17], and tibia defects [39]. However, fibrin hydrogels present shortcomings

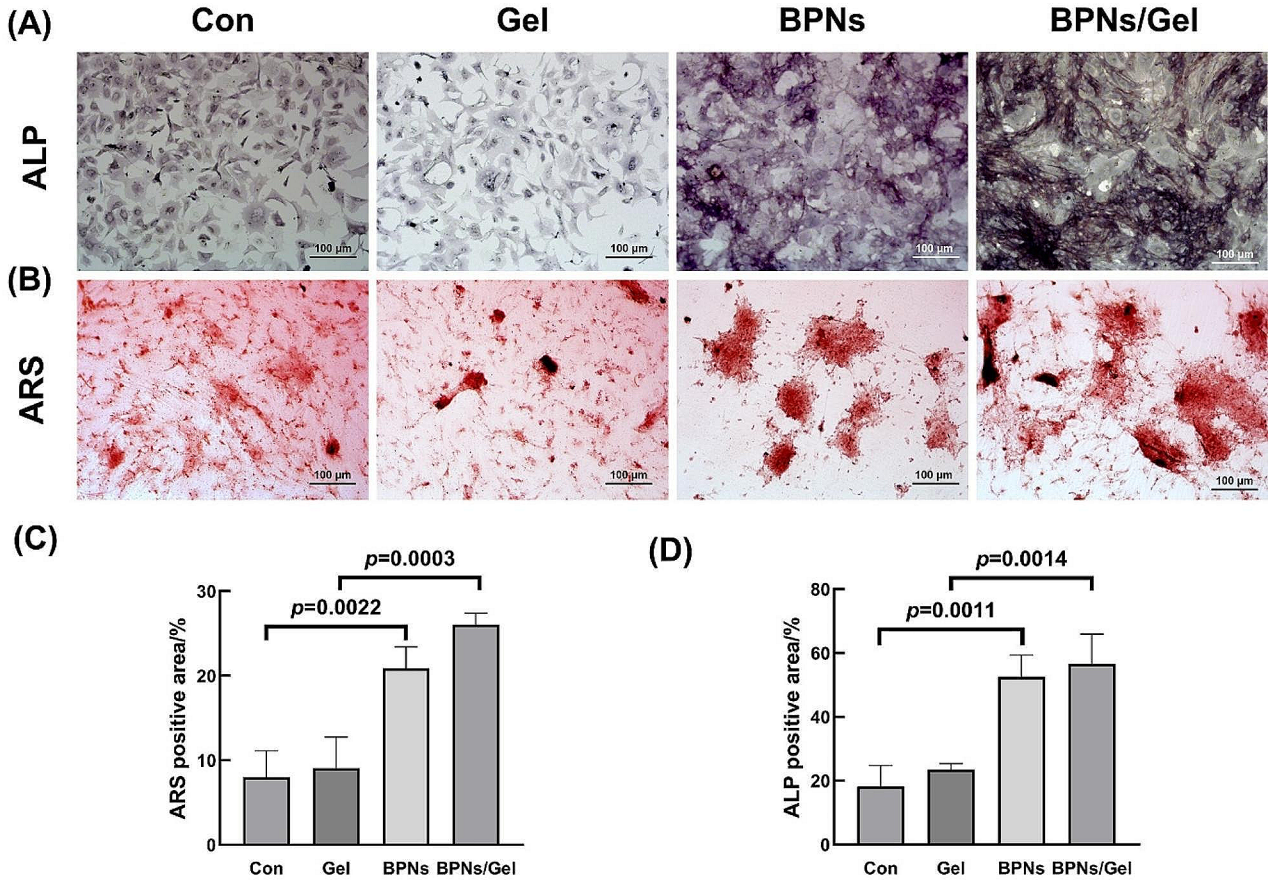

Fig. 6 The osteogenic differentiation of EMSCs on fibrin-KGM hydrogels or BPNs/fibrin-KGM hydrogels. **(A)** Alkaline phosphatase staining of EMSCs cultured for 7 days. Image Pro was used to evaluate the percentage of positive areas. **(B)** The calcium depositions of the osteogenesis-induced EMSCs were dyed by Alizarin Red S staining. (**C**, **D**) ALP and ASR positive area of the total analysis area of the region. Data were presented as mean ± standard deviation (SD), $n = 3$

such as rapid degradation and weak mechanical properties, which limit their further application in bone tissue engineering. The degradation rate of the hydrogels should at least match the forming rate of new bone tissue [40], to meet the requirements of an ideal scaffold for bone regeneration. How to delay the degradation of fibrin hydrogels to better adapt to the long-term process of bone repair is an urgent problem to be solved.

As a natural polysaccharide extracted from Konjac, KGM possesses excellent gel properties after deacetylation [24]. The application of KGM has been extended from food to biomaterial fields in recent years. Kondo and his colleagues [41] used KGM and hyaluronic acid (HA) as scaffolds for cartilage regeneration and found the cell viability of chondrocytes in KGM/HA hydrogels was higher than that in agarose hydrogels, demonstrating the potential of KGM in medical and pharmaceutical areas. In this study, the addition of KGM greatly slowed down the degradation rates of fibrinogen hydrogels, improved the mechanical properties, and promoted cell proliferation. KGM can combine with protein by the aggregation of hydroxyl groups, strong hydrogen bonding interactions [42], or the Maillard reaction between the hydroxyl groups of KGM and amino groups of protein [43], and form composite gels with lower degradation rates and better mechanical properties. KGM/fibrin hydrogels can simulate the structure of the extracellular matrix and provide a fine extracellular environment for the growth of stem cells, thus promoting cell survival and proliferation.

Phosphate plays an important role in bone regeneration. The BPNs are an emerging 2D material with biocompatibility and the ability to continuously release phosphate ions [44]. In this study, the BPNs were prepared from bulk BP by liquid exfoliation. SEM images and the determination of particle size distribution illustrated the successful preparation of BPNs. According to our previous study, 4 μg/mL BPNs were biocompatible and were able to promote the osteogenesis of EMSCs effectively. Thus, BPNs at a concentration of 4 μg/mL was chosen in this study. BPNs at a concentration higher than 64 μg/mL exhibited cytotoxicity [26]. In addition, BPNs at a high concentration also had an impact on the

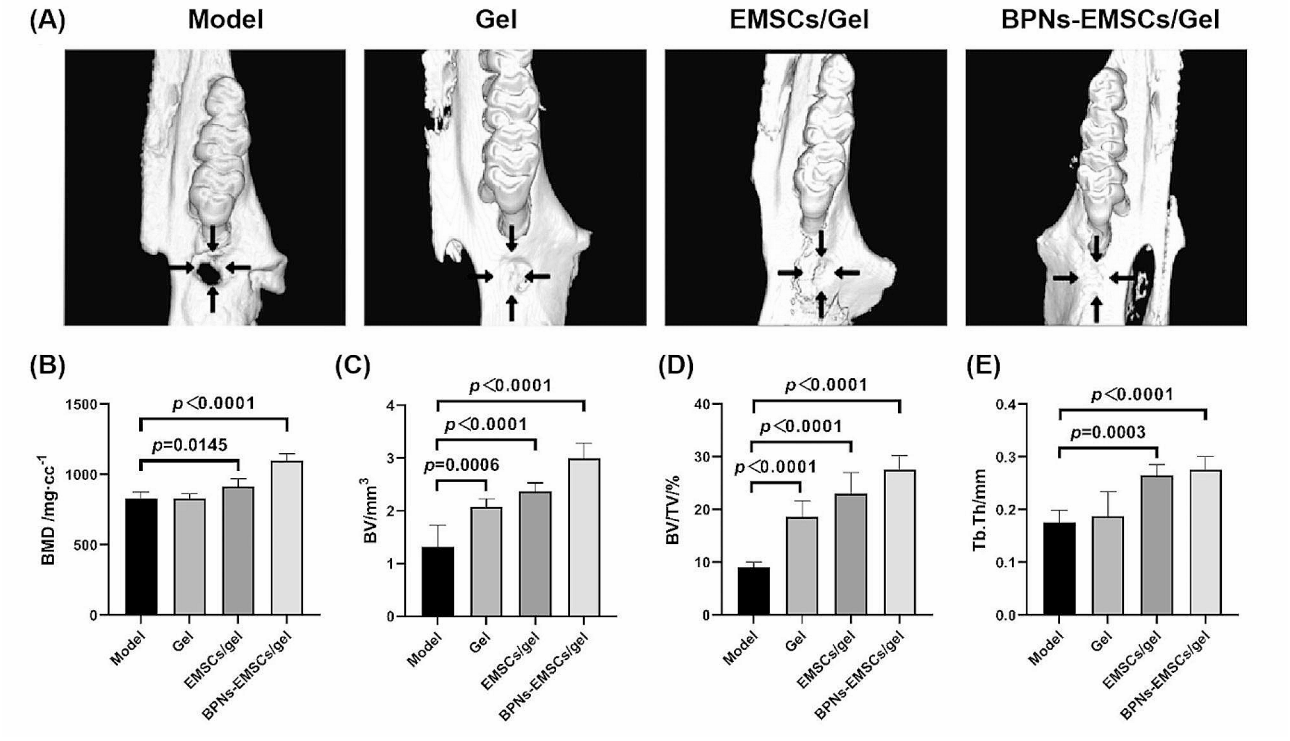

Fig. 7 Micro-CT analysis of alveolar bone defect rats. **(A)** The three-dimensional reconstruction of the maxillary bone tissues of the bone-defect rats, treated with hydrogels, EMSCs-containing hydrogels, and BPNs/EMSCs-containing hydrogels. The defect area was pointed by the black arrows. (**B**-**E**) Quantitative analysis of the maxillary bone tissues. Data were presented as mean ± SD, $n = 6$

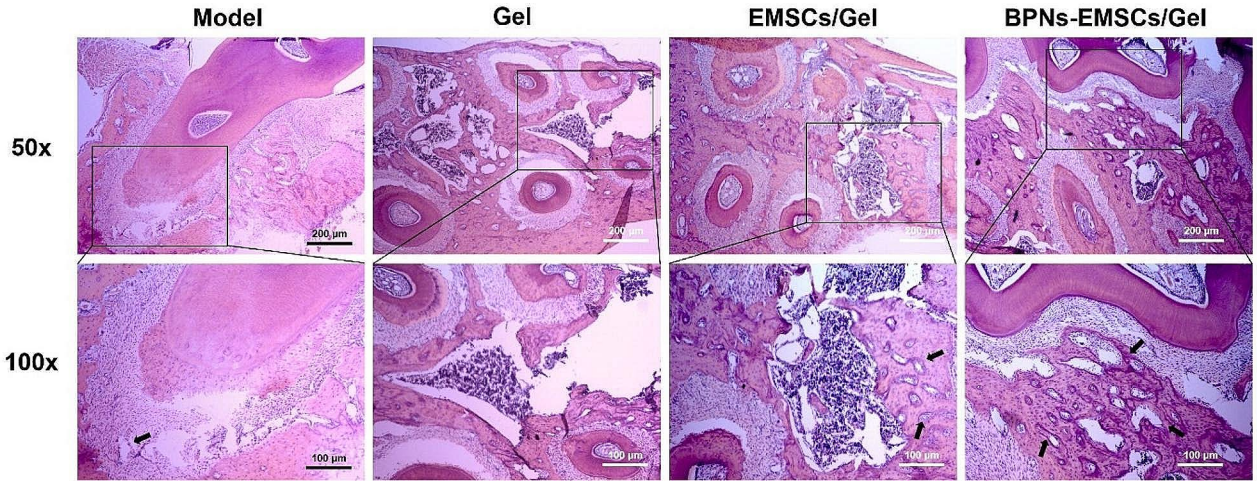

Fig. 8 Histological analysis of the alveolar bone defect area. H&E staining was performed to determine the bone regeneration (50× and 100×). The black arrows pointed to the newly formed vessels

mechanical properties of the hydrogels including swelling ratios and compression modulus of the hydrogels [40]. However, our results indicated that 4 μg/mL BPNs did not affect the gel properties and biocompatibility of the composite hydrogels, and can also effectively promote the osteogenesis of EMSCs. On the one hand, BPNs can release phosphate ions sustainedly, trapping Ca^{2+} to promote the formation of calcium phosphate and new bone [45]. Besides, BPNs can upregulate the expression of transglutaminase 2 (TG2) to accelerate the osteogenic differentiation of EMSCs [26]. TG2 could bind to its target substrates including COL, OPN, fibronectin, and bone sialoprotein [46], and promote the formation of bone matrix [47]. Furthermore, TG2 also possesses ATPase activity and can contribute to improving the levels of Pi, which are essential to mineral deposition [48].

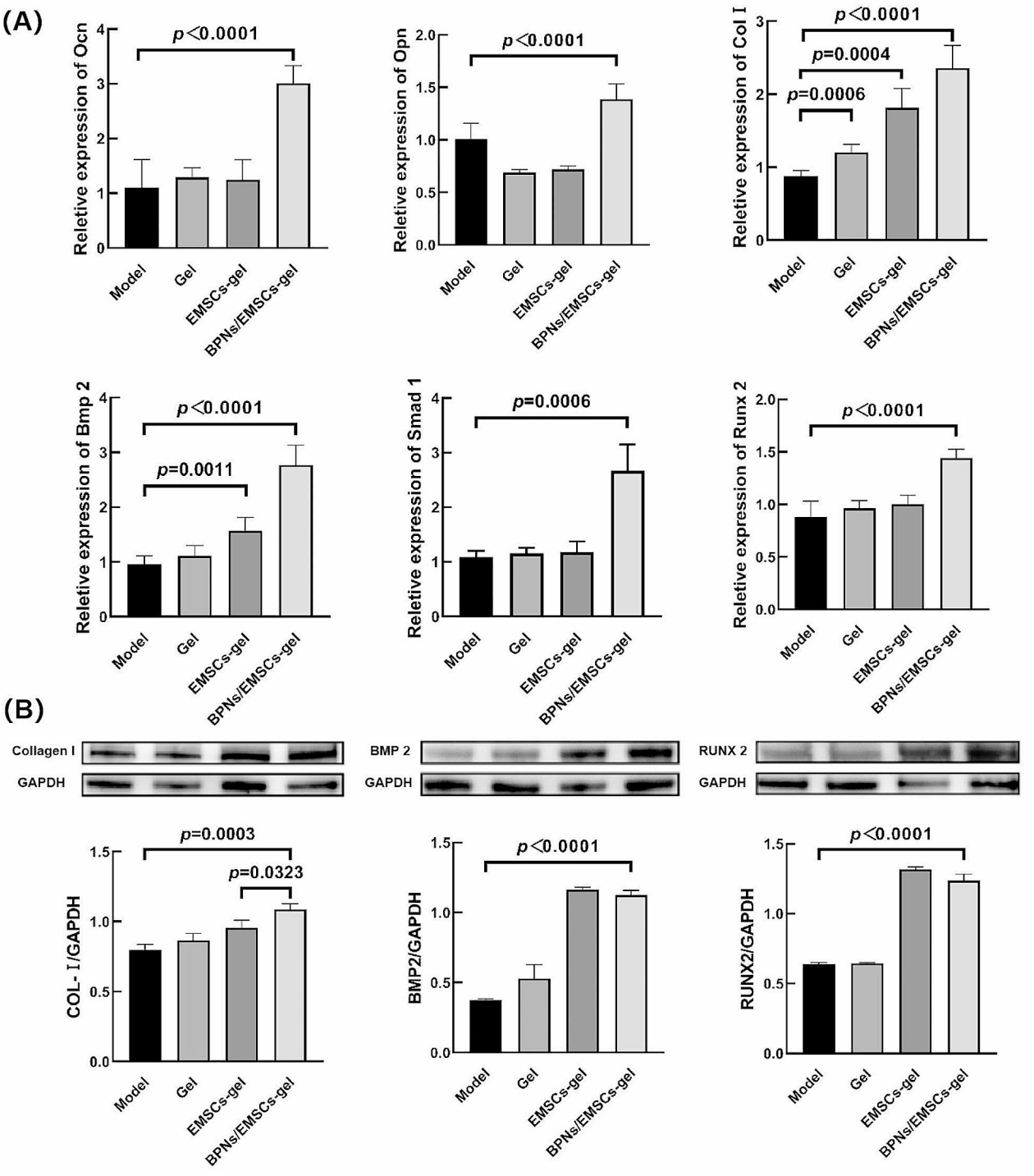

Fig. 9 Osteogenesis-related mRNA and protein expression. **(A)**The osteogenesis-related mRNA expression of *Ocn*, *Opn*, *Col*, *Bmp2*, *Smad1* and *Runx2*. **(B)**The protein expression levels of COL, BMP2, and RUNX2 were analyzed by western blotting. Data were presented as mean ± SD, $n = 3$

To verify the bone regeneration effects of the EMSCs-loaded composite hydrogels, the alveolar bone defect model of rats was conducted. The micro-CT and histological analysis indicated that the repair effects of EMSCs/gel and BPNs-EMSCs/gel were better than that of the model group and hydrogel group. The role of BPNs-containing hydrogels in accelerating bone reconstruction in vivo could be supporting the adhesion and proliferation of EMSCs, and the activation of the BMP/Smad pathway.

BMP2 is a key regulator in bone tissue formation that regulates the osteogenic differentiation of mesenchymal

stem cells [49]. BMP 2 is bound to its receptor on the cell membrane to activate the phosphorylation of SMAD1, SMAD5, or SMAD8 in cells [50]. The activated Smad family can be transferred from the cytoplasm to the nucleus, or act on downstream target genes to activate the transcription of specific target genes such as *Runx2* [51–53]. RUNX2 can regulate the transcription of different genes such as osteocalcin, bone salivary protein, and other signaling proteins for bone turnover [54]. It was worth noting that the mRNA expression levels of *Bmp2*, *Smad1*, and *Runx2* were significantly upregulated in the BPNs-EMSCs/gel group ($p<0.01$), while no similar results were observed in the EMSCs/gel group. Therefore, the results indicated the possibility that the BPNs-containing composite hydrogels could induce the activation of the BMP/Smad pathway to accelerate the reconstruction of bone tissues. In addition to differentiating into osteoblasts, EMSCs can also promote bone repair by secreting cytokines, growth factors, and extracellular matrix glycoproteins [55]. In this study, ECM gene markers including *Ocn*, *Opn*, and *Col* were all upregulated in the BPNs-EMSCs/gel group ($p<0.05$).

Although the results of this study presented significant differences in the repair of alveolar bone defects by BPNs/fibrin-KGM-EMSCs composite hydrogels, there are still some limitations. Further investigation is needed to illustrate the specific molecular mechanism of the repair effects on alveolar bone defects. In the future, the potential of BPNs/fibrin-KGM-EMSCs hydrogels in the treatment of clinical alveolar bone defects needs to be further explored by large animal experiments to determine the efficacy and safety of this hydrogel.

Conclusions

In this work, EMSCs/BPNs-containing fibrin-KGM hydrogels were prepared and characterized as scaffolds for bone tissue engineering, and the treatment effects were evaluated by the alveolar bone defect model in rats. The addition of KGM improved the mechanical properties, water-holding capacity, and biodegradation characteristics of pure fibrin hydrogels, promoting the proliferation of EMSCs. The BPNs-containing compound hydrogel was proved to be capable of enhancing the osteogenesis of EMSCs. In addition, BPNs/fibrin-KGM composite scaffolds loaded with EMSCs could effectively up-regulate the expression of osteogenic-related genes, promote the formation and mineralization of bone matrix, and accelerate the repair process of alveolar bone defect in rats. Taken together, the EMSCs/BPNs-containing compound hydrogel is a promising candidate in the repair of alveolar bone defects induced by oral diseases such as periodontitis, tumors, orthodontic, and cysts, etc.

Abbreviations

ALP	Alkaline phosphatase
ARS	Alizarin red S
BPNs	Black phosphorus nanoparticles
Calcein-AM and PI	Calcein acetoxymethyl ester and propidium iodide
CCK-8	Cell Counting Kit-8
Col	Type collagen
DMEM	Dulbecco's modified Eagle's medium/nutrient mixture
EMSCs	Ectodermal mesenchymal stem cells
FITC	Fluorescein isothiocyanate
Gapdh	Glyceraldehyde-3-phosphate dehydrogenase
H&E Staining	Hematoxylin-eosin staining
KGM	Konjac glucomannan
micro-CT	Micro-computed tomography
Opn	Osteopontin
Ocn<	Osteocalcin
PBS	Phosphate buffer saline
RT-qPCR	Real-time quantitative polymerase chain reaction
Runx 2	Runt-related transcription factor 2
SD	Standard deviation
SEM	Scanning electron microscope
WHC	Water-holding capacity

Supplementary Information

The online version contains supplementary material available at https://doi.org/10.1186/s12903-024-04649-0.

Supplementary Material 1

Acknowledgements

We thank the drawing tools provided by Figdraw (www.figdraw. com).

Author contributions

YZ, WX and N-YL, conceptualization and methodology. YZ, XM and X-HW, investigation , data curation, formal analysis and writing-original draft. XZ, validation. XW and WX, supervision. WX and N-YL, writing-review and editing, project administration, and acquisition. All authors contributed to the article and approved the submitted version. N-YL is the corresponding author. All authors have read and approved the final manuscript.

Funding

This work was supported by the Top Talent Support Program for young and middle-aged people of Wuxi Health Committee (No. HB2023093) and the Young project of the Wuxi Health Committee (No. Q202102).

Data availability

The datasets generated during and/or analyzed during the study are available from the corresponding author upon reasonable request.

Declarations

Ethics approval and consent to participate

All the animal procedures were approved by Jiangnan University Animal Care and Ethics Committee (JN.No20220430S04206130[143]) and were performed in accordance with the International Guidelines for Animal Research in this study.

Consent for publication

Not applicable.

Competing interests

The authors declare no competing interests.

Author details

[1]Department of Stomatology, Affiliated Children's Hospital of Jiangnan University, Jiangnan University, Wuxi, Jiangsu Province, People's Republic of China

[2]School of Food Science and Technology, Jiangnan University, Wuxi, Jiangsu Province, People's Republic of China
[3]Jiangnan University Medical Center, Wuxi, Jiangsu Province, People's Republic of China
[4]Department of Hepatobiliary Surgery, Affiliated Hospital of Jiangnan University, Wuxi, Jiangsu Province, People's Republic of China

Received: 4 March 2024 / Accepted: 23 July 2024
Published online: 02 August 2024

References

1. Foster BL, Nociti FH Jr., Somerman MJ. Rachitic Tooth Endocr Reviews. 2014;35(1):1–34.
2. Haggerty CJ, Vogel CT, Fisher GR. Simple bone augmentation for Alveolar Ridge defects. Oral Maxillofac Surg Clin N Am. 2015;27(2):203–26.
3. Dimitriou R, Jones E, McGonagle D, Giannoudis PV. Bone regeneration: current concepts and future directions. BMC Med. 2011;9:66.
4. Giannoudis PV, Dinopoulos H, Tsiridis E. Bone substitutes: an update. Injury-Int J Care Inj. 2005;36:20–7.
5. Ahlmann E, Patzakis M, Roidis N, Shepherd L, Holtom P. Comparison of anterior and posterior iliac crest bone grafts in terms of harvest-site morbidity and functional outcomes. J Bone Joint Surgery-American Volume. 2002;84A(5):716–20.
6. Baldwin P, Li DJ, Auston DA, Mir HS, Yoon RS, Koval II. Autograft, Allograft, and bone graft substitutes: clinical evidence and indications for Use in the setting of Orthopaedic Trauma surgery. J Orthop Trauma. 2019;33(4):203–13.
7. Stevenson S, Horowitz M. The response to bone allografts. J Bone Joint Surgery-American Volume. 1992;74A(6):939–50.
8. Dibbs RP, Ferry AM, Sarrami SM, Abu-Ghname A, Dempsey RF, Buchanan EP. Distraction osteogenesis: Mandible and Maxilla. Facial Plast Surg. 2021;37(06):751–8.
9. Efunkoya AA, Bamgbose BO, Adebola RA, Adeoye JB, Akpasa IO. Maxillomandibular Distraction Osteogenesis. J Craniofac Surg. 2014;25(5):1787–92.
10. Hurmerinta K, Peltomaki T, Hukki J. Unexpected events during mandibular distraction osteogenesis. Scand J Plast Reconstr Surg Hand Surg. 2004;38(4):209–14.
11. Henkel J, Woodruff MA, Epari DR, Steck R, Glatt V, Dickinson IC, et al. Bone regeneration based on tissue Engineering conceptions - A 21st Century Perspective. Bone Res. 2013;1:216–48.
12. Perez JR, Kouroupis D, Li DJ, Best TM, Kaplan L, Correa D. Tissue Engineering and Cell-based therapies for fractures and bone defects. Front Bioeng Biotechnol. 2018;6:105.
13. Noori A, Ashrafi SJ, Vaez-Ghaemi R, Hatamian-Zaremi A, Webster TJ. A review of fibrin and fibrin composites for bone tissue engineering. Int J Nanomed. 2017;12:4937–61.
14. Salhotra A, Shah HN, Levi B, Longaker MT. Mechanisms of bone development and repair. Nat Rev Mol Cell Biol. 2020;21(11):696–711.
15. Li FF, Li S, Liu Y, Zhang ZT, Li ZJ. Current advances in the roles of Doped Bioactive Metal in Biodegradable Polymer Composite scaffolds for bone repair: a Mini Review. Adv Eng Mater. 2022;24(8).
16. Fontaine ML, Combes C, Sillam T, Dechambre G, Rey C. New calcium carbonate-based cements for bone reconstruction. In: Li P, Zhang K, Colwell CW, editors. Bioceramics 17. Key Engineering Materials. 284-2862005. pp. 105-8.
17. Le Guehennec L, Goyenvalle E, Aguado E, Pilet P, D'Arc MB, Bilban M, et al. MBCP biphasic calcium phosphate granules and tissucol sealant in rabbit femoral defects: the effect of fibrin on bone ingrowth. J Mater Science-Materials Med. 2005;16(1):29–35.
18. Latiff NM, Mayorga-Martinez CC, Sofer Z, Fisher AC, Pumera M. Cytotoxicity of phosphorus allotropes (black, violet, red). Appl Mater Today. 2018;13:310–9.
19. Shi WT, Que YD, Zhang X, Bian L, Yu XJ, Tang X et al. Functional tissue-engineered bone-like graft made of a fibrin scaffold and TG2 gene-modified EMSCs for bone defect repair. Npg Asia Mater. 2021;13(1).
20. Delorme B, Nivet E, Gaillard J, Häupl T, Ringe J, Devèze A, et al. The Human Nose harbors a niche of olfactory ectomesenchymal stem cells displaying Neurogenic and Osteogenic properties. Stem Cells Dev. 2010;19(6):853–66.
21. Xiang W, Wang X, Yu X, Xie Y, Zhang L, Lu N, et al. Therapeutic efficiency of nasal mucosa-derived ectodermal mesenchymal stem cells in rats with Acute hepatic failure. Stem Cells Int. 2023;2023(1):6890299.
22. Jafri MA, Kalamegam G, Abbas M, Al-Kaff M, Ahmed F, Bakhashab S et al. Deciphering the Association of Cytokines, chemokines, and growth factors in Chondrogenic differentiation of human bone marrow mesenchymal stem cells using an ex vivo Osteochondral Culture System. Front Cell Dev Biology. 2020;7.
23. Shi W, Que Y, Zhang X, Bian L, Yu X, Tang X et al. Functional tissue-engineered bone-like graft made of a fibrin scaffold and TG2 gene-modified EMSCs for bone defect repair. NPG Asia Mater. 2021;13(1).
24. Williams MAK, Foster TJ, Martin DR, Norton IT, Yoshimura M, Nishinari K. A molecular description of the gelation mechanism of Konjac Mannan. Biomacromolecules. 2000;1(3):440–50.
25. Zhang YQ, Xie BJ, Gan X. Advance in the applications of Konjac Glucomannan and its derivatives. Carbohydr Polym. 2005;60(1):27–31.
26. Lu NY, Wang XH, Shi WT, Bian L, Zhang X, Yang GF et al. Black Phosphorus nanoparticles promote osteogenic differentiation of EMSCs through upregulated TG2 expression. Nanoscale Res Lett. 2021;16(1).
27. Xia FN, Wang H, Jia YC. Rediscovering black phosphorus as an anisotropic layered material for optoelectronics and electronics. Nat Commun. 2014;5.
28. Shimahara H, Suzuki H, Sugiyama N, Nisizawa K. Partial purification of beta-mannanases from the konjac tubers and their substrate specificity in relation to the structure of Konjac Glucomannan. Agric Biol Chem. 1975;39(2):301–12.
29. Fan R, Ma PH, Zhou D, Yuan F, Cao XL. The properties and formation mechanism of oat beta-glucan mixed gels with different molecular weight composition induced by high-pressure processing. PLoS ONE. 2019;14(12).
30. Liang Y, Wen L, Shang F, Wu J, Sui K, Ding Y. Endothelial progenitors enhanced the osteogenic capacities of mesenchymal stem cells in vitro and in a rat alveolar bone defect model. Arch Oral Biol. 2016;68:123–30.
31. Ho-Shui-Ling A, Bolander J, Rustom LE, Johnson AW, Luyten FP, Picart C. Bone regeneration strategies: Engineered scaffolds, bioactive molecules and stem cells current stage and future perspectives. Biomaterials. 2018;180:143–62.
32. Bongio M, van den Beucken J, Leeuwenburgh SCG, Jansen JA. Development of bone substitute materials: from 'biocompatible' to 'instructive'. J Mater Chem. 2010;20(40):8747–59.
33. Babis GC, Soucacos PN. Bone scaffolds: the role of mechanical stability and instrumentation. Injury-Int J Care Inj. 2005;36:S38–44.
34. Jeong J, Kim JH, Shim JH, Hwang NS, Heo CY. Bioactive calcium phosphate materials and applications in bone regeneration. Biomater Res. 2019;23:4.
35. Szpalski C, Wetterau M, Barr J, Warren SM. Bone tissue Engineering: current strategies and techniques-part I: scaffolds. Tissue Eng Part B-Reviews. 2012;18(4):246–57.
36. Breen A, O'Brien T, Pandit A. Fibrin as a delivery system for therapeutic drugs and biomolecules. Tissue Eng Part B-Reviews. 2009;15(2):201–14.
37. Linsley CS, Wu BM, Tawil B. Mesenchymal stem cell growth on and mechanical properties of fibrin-based biomimetic bone scaffolds. J Biomedical Mater Res Part A. 2016;104(12):2945–53.
38. Arnaud E, Morieux C, Wybier M, Devernejoul MC. Potentiation of transforming growth-factor (TGF-β-1) by natural coral and fibrin in a rabbit Cranioplasty Model. Calcif Tissue Int. 1994;54(6):493–8.
39. Kalia P, Blunn GW, Miller J, Bhalla A, Wiseman M, Coathup MJ. Do autologous mesenchymal stem cells augment bone growth and contact to massive bone tumor implants? Tissue Eng. 2006;12(6):1617–26.
40. Huang K, Wu J, Gu Z. Black Phosphorus Hydrogel scaffolds enhance bone regeneration via a sustained supply of calcium-free phosphorus. ACS Appl Mater Interfaces. 2019;11(3):2908–16.
41. Kondo T, Shinozaki T, Oku H, Takigami S, Takagishi K. Konjac Glucomannan-based hydrogel with hyaluronic acid as a candidate for a novel scaffold for chondrocyte culture. J Tissue Eng Regen Med. 2009;3(5):361–7.
42. Wang L, Xiao M, Dai SH, Song J, Ni XW, Fang YP, et al. Interactions between carboxymethyl konjac glucomannan and soy protein isolate in blended films. Carbohydr Polym. 2014;101:136–45.
43. Wang K, Wu K, Xiao M, Kuang Y, Corke H, Ni XW, et al. Structural characterization and properties of konjac glucomannan and zein blend films. Int J Biol Macromol. 2017;105:1096–104.
44. Ling X, Wang H, Huang SX, Xia FN, Dresselhaus MS. The renaissance of black phosphorus. Proc Natl Acad Sci USA. 2015;112(15):4523–30.
45. Cai YR, Tang RK. Calcium phosphate nanoparticles in biomineralization and biomaterials. J Mater Chem. 2008;18(32):3775–87.
46. Telci D, Collighan RJ, Basaga H, Griffin M. Increased TG2 expression can result in induction of transforming growth factor beta 1, causing increased synthesis and deposition of Matrix proteins, which can be regulated by nitric oxide. J Biol Chem. 2009;284(43):29547–58.

47. Al-Jallad HF, Nakano Y, Chen JLY, McMillan E, Lefebvre C, Kaartinen MT. Transglutaminase activity regulates osteoblast differentiation and matrix mineralization in MOT3-E1 osteoblast cultures. Matrix Biol. 2006;25(3):135–48.
48. Nakano Y, Forsprecher J, Kaartinen MT. Regulation of ATPase activity of transglutaminase 2 by MT1-MMP: implications for mineralization of MC3T3-E1 osteoblast cultures. J Cell Physiol. 2010;223(1):260–9.
49. Zhu LW, Liu YZ, Wang A, Zhu ZQ, Li YB, Zhu CY et al. Application of BMP in bone tissue Engineering. Front Bioeng Biotechnol. 2022;10.
50. Cheng W, Yang SF, Liang F, Wang W, Zhou R, Li Y, et al. Low-dose exposure to triclosan disrupted osteogenic differentiation of mouse embryonic stem cells via BMP/ERK/Smad/Runx-2 signalling pathway. Food Chem Toxicol. 2019;127:1–10.
51. Zou ML, Chen ZH, Teng YY, Liu SY, Jia Y, Zhang KW et al. The smad dependent TGF-beta and BMP signaling pathway in bone remodeling and therapies. Front Mol Biosci. 2021;8.
52. Wu MR, Chen GQ, Li YP. TGF-beta and BMP signaling in osteoblast, skeletal development, and bone formation, homeostasis and disease. Bone Res. 2016;4:272–88.
53. Mei W, Xu C. BMP signaling in skeletal development. Biochem Biophys Res Commun. 2005;328(3):651–7.
54. Lian JB, Stein GS, Javed A, van Wijnen AJ, Stein JL, Montecino M, et al. Networks and hubs for the transcriptional control of osteoblastogenesis. Reviews Endocr Metabolic Disorders. 2006;7(1–2):1–16.
55. Liu H, Peng H, Wu Y, Zhang C, Cai Y, Xu G, et al. The promotion of bone regeneration by nanofibrous hydroxyapatite/chitosan scaffolds by effects on integrin-BMP/Smad signaling pathway in BMSCs. Biomaterials. 2013;34(18):4404–17.

Publisher's Note